Proton Magnetic Relaxation Studies of Various Guest Molecules in Clathrate Hydrates

Doris M. Jacobs and Manfred D. Zeidler*

Institut für Physikalische Chemie, Rheinisch-Westfälische Technische Hochschule Aachen, Templergraben 59, D-52056 Aachen, Germany

Otmar Kanert

Institut für Experimentelle Physik, Universität Dortmund, Otto-Hahn-Str. 4, D-44227 Dortmund, Germany

Received: January 29, 1997; In Final Form: May 9, 1997[⊗]

The rotational dynamics of guest molecules in clathrate hydrates is studied by varying both the cage geometries of the host lattice and the properties of the cyclic guest species, as dipole moments, diameters, and moments of inertia. Proton spin−lattice relaxation rates have been obtained over a temperature range 20−263 K. The relaxation is caused by intramolecular dipole−dipole interactions only. The asymmetric relaxation rate versus inverse temperature curves have been fitted by using the Davidson−Cole spectral density $J(\omega\tau, \beta)$. Shape parameters β between 0.1 and 0.3 are found for the reorientation of guests in their cages. Correlation times lying between 2.57×10^{-12} and 4.97×10^{-10} s and low activation energies indicate high guest mobility due to weak van der Waals interactions between guest and host. The reorientation of the guest molecules depends on the different cage types and guest geometries as well. The motions are specific for each cage type. For different guest molecules in the same cage type the correlation times increase with increasing diameters and moments of inertia of the molecules.

Introduction

Clathrate hydrates[1,2] are nonstoichiometric compounds consisting of guest molecules and host water molecules. The latter molecules form a three-dimensional hydrogen-bonded network similar to the network of various ice polymorphs. The guest molecules are accommodated in the well-defined cages of the host lattice.

Clathrate hydrates are only stable with guest molecules. The interactions between guest and water molecules are mainly based on van der Waals forces. The formation and stability of clathrate hydrates depend to a large extent on the size and shape of guest molecules as well as on temperature and pressure conditions. Gases such as H_2S or N_2 are often used to compensate the stability loss due to the presence of large guests whose sizes are close to the upper limit of the cage radius. Besides the guest size and cage occupancy, the dynamical behavior of the host and guest molecules plays a key role in controlling the stability of clathrate hydrates.[3]

Van Stackelberg et al.[4,5] have shown that clathrate hydrates are generally classified into two different hydrate crystal structures. Structure I forms a cubic body-centered unit cell of space group *Pm*3*n* and has a lattice parameter of 12.0 Å. It is composed of two pentagonal dodecahedra and six tetrakaidecahedra connected by edges. If all cavities are occupied by the guest compounds X and Y, the ideal unit cell formula is $6X{\cdot}2Y{\cdot}46H_2O$. (X and Y refer to guest molecules in the tetrakaidecahedra and in the dodecahedra, respectively.) Structure II forms a cubic face-centered unit cell of space group *Fd*3*m* and has a lattice parameter of 17.3 Å. It consists of 16 pentagonal dodecahedra and 8 hexakaidecahedra connected by their faces. A complete occupancy of the cavities results in an ideal unit cell formula of $8X{\cdot}16Y{\cdot}136H_2O$.

The pentagonal dodecahedron (5^{12}) is the smallest cavity with an average radius of 3.90 Å. The crystal symmetry of this cage is different in structures I and II. The tetrakaidecahedron ($5^{12}6^2$) with an average radius of 4.33 Å is composed of 12 pentagonal and 2 hexagonal faces. Because of its distorted cubic symmetry ($\bar{4}2m$), this cage represents an oblate spheroid possessing one unique axis. The largest cavity is the hexakaidecahedron with an average radius of 6.6 Å. It has 12 pentagonal and 4 hexagonal faces. This cavity is nearly spherical with a variation of 2% in radius, whereas in the tetrakaidecahedron the distances between the oxygen atoms and the center of the cage vary at an average of 14%. The cage symmetries have important consequences with respect to the motions and NMR properties of guest species.[6]

The dynamics of the guest molecules are restricted to rotational motions. NMR proton relaxation is a suitable technique for studying these motions. Disturbing signals from water molecules are avoided by preparing the clathrates with deuterium oxide. The motions of the guest molecules tetrahydrofuran,[7−9] trimethylene oxide,[10] and cyclobutanone[10] in the corresponding clathrate hydrates $1THF{:}17D_2O$, $1TMO{:}7^2/_3D_2O$, and $1CB{:}17D_2O$ have been studied previously by NMR proton relaxation. The relaxation rate versus inverse temperature curves, which have been measured over a wide temperature range (10−273 K), show asymmetric shapes. The fit parameters of these curves clearly indicate high guest mobility due to low activation energies. According to Davidson,[11] the rotational mobility of guest molecules depends both on geometric factors (the size and shape of the guest molecule with respect to the cage) and on the interaction of the dipole moment of the guest molecule with the electrostatic fields of the water molecules. To examine the influence of molecular properties of the guests on their reorientation, we present here results of NMR studies of several guest molecules in clathrate hydrates (mainly of structure II) in which either the guest species or the cavity types are varied. The cyclic compounds tetrahydrofuran (THF), 1,3-dioxolane (DX), cyclopentane (CP), cyclobutanone (CB), propylene oxide (PO), and trimethylene oxide (TMO) were selected as guest molecules in the hexakaidecahedra of structure II. TMO was also encaged in the tetrakaidecahedra of structure I.

[⊗] Abstract published in *Advance ACS Abstracts,* June 15, 1997.

S1089-5639(97)00353-8 CCC: $14.00

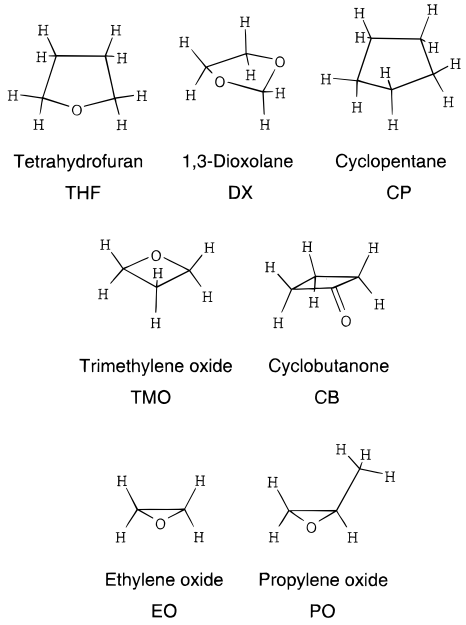

Figure 1. Guest molecules.

Ethylene oxide (EO) was enclathrated in the tetrakaidecahedra of structure I and in the pentagonal dodecahedra of structure II. The guest molecules are shown in Figure 1. When the relaxation rates of each clathrate hydrate under the same conditions (20−156 K at 60 MHz and 140−263 K at 300 MHz) are measured, the different reorientational behavior of the guests can be directly compared with each other and referred to molecule-dependent properties as dipole moments, diameters, and moments of inertia.

Experimental Section

Nine different clathrate hydrates were prepared (see Table 1). Water (99.95% D_2O) and the guest were weighted to the exact mole fractions separately and to 0.1% accuracy. Oxygen was then removed from the samples in five freeze−pump−thaw cycles under a pressure of 10^{-6} bar. The liquids were subsequently condensed in an NMR tube, whereby water was transferred first. For the ternary mixtures EO was condensed last. After sealing the tube, the substances were thawed and mixed.

For the clathrates PO(II), TMO(II), CB(II), and DX(II), whose melting points are lower than 4 °C, a complete crystallization was achieved by partially thawing and freezing the samples. During this process the samples had to be shaken thoroughly in order to avoid formation of ice. Pure crystals of the clathrate TMO(I) were formed by fast cooling of the mixture with liquid nitrogen and subsequent tempering at −30 °C. After about 5 weeks the crystallization process was completed.

The aqueous mixtures with EO, CP, TDF/EO (TDF: deuterated THF), and THF/EO_d (EO_d: deuterated EO) crystallized as clathrates at a temperature of 2 ± 1 °C within 1 week. Nucleation was induced by occasionally shaking the samples and dipping them shortly into liquid nitrogen.

A complete crystallization of the double clathrates was obtained with a stoichiometry of 1THF:0.5EO_d:17D_2O or 1TDF:0.5EO:17D_2O, respectively.[12] The deviation from the ideal cell formula of 1:3:17 is attributed to the large diameter ratio of about 1.06 for EO in the pentagonal dodecahedra. Consequently, only 12% of the small cavities are occupied by EO molecules.

The melting points are at most 4 °C higher than the literature data referring to clathrates with protonated host lattices. This discrepancy may originate from the use of D_2O, the melting point of which is also 4 °C higher than that of H_2O, and from the renunciation of help gas during the preparation.

The clathrate hydrates were identified by X-ray diffraction. The diffraction patterns were obtained with a Guinier camera G645 (Cu Kα1 radiation, Ge-crystal monochromator) at 143 K over an angular range of $4° \leq \theta \leq 30°$. They were indexed according to the space groups *Fd*3*m* for structure II and *Pm*3*n* for structure I.

The lattice constants (see Table 1) are in excellent agreement with the literature data. In accordance with Sargent and Clavert[13] we found that the diffraction pattern of the clathrate TMO(II) includes reflexes of structure II as well as of structure I. We assume that TMO is enclathrated in the hexakaidecahedra and in the tetrakaidecahedra as well because this guest molecule is the smallest molecule known to occupy the large cavities of structure II. We also observed that the diffraction patterns measured at 243 K contain impurities of ice reflexes, whereas the patterns obtained at 143 K consist of clathrate reflexes only.

Relaxation times T_1 were measured over a temperature range 20−263 K at the spectrometer frequencies $\omega_0 = 300.13$ MHz (140−263 K) and $\omega_0 = 60$ MHz (20−156 K). For the 300 MHz spectrometer low-temperature (<140 K) equipment was unfortunately not available. In the temperature region 50−263 K T_1 measurements were done using the inversion−recovery method ($180°-\tau-90°$). The saturation recovery sequence ($(90°-\tau_i)_n-\tau-90°$; $\tau_{i+1} = \tau_i/2 = 2 - 3T_2$) was employed in the temperature region 20−50 K. The reproducibility of the T_1 data was 3%, and the temperature control was within 1 K.

Theory

For the nine different clathrates the temperature dependencies of the relaxation rates are shown in Figures 2−7. The data were fitted by using the equation for the intramolecular dipole−dipole interaction because this relaxation mechanism is the only contribution to the relaxation at low temperatures. According to Albayrak et al.,[7] the intermolecular dipole−dipole interaction can be neglected. The relaxation rate $1/T_1$ depends on the coupling constant C, the generalized order parameter s^2, and the spectral density j_{CD}:

$$\left(\frac{1}{T_1}\right)^{H}_{DD,intra} = Cs^2\{j_{CD}(\omega_0) + 4j_{CD}(2\omega_0)\} \qquad (1)$$

The structure parameter C is given by

$$C = \frac{3}{10}\gamma^4\hbar^2\left(\frac{\mu_0}{4\pi}\right)^2\left\langle\frac{1}{r^6}\right\rangle \qquad (2)$$

where μ_0, γ, and $\hbar$ are the vacuum permeability, the proton gyromagnetic ratio, and the Planck's constant, respectively. The average proton−proton distance is calculated from all pair interactions of the single dipoles normalized to the total number N of relaxing nuclei in the molecule:

$$\left\langle\frac{1}{r^6}\right\rangle = \frac{1}{N}\sum_{i=1}^{N}\sum_{\substack{j=1\\ j\neq i}}^{N}\frac{1}{r_{ij}^6} \qquad (3)$$

By reference to the guest molecules presented in this paper, the primary contribution arises from geminal protons of a methylen group. Since proton−proton distances of 2.0−2.5 Å contribute on average 20% to the relaxation, the nearest vicinal protons also have to be considered. Protons that are 3 Å apart only have small influence on the relaxation rate. Because protons with different chemical shifts are not resolved, all

TABLE 1: Melting Points (*T*) and Lattice Parameters (*a*) of the Prepared Clathrates

name	clathrate	stoichiometry	*T* (expt)/°C	*T* (lit)/°C	*a* (expt)/Å	*a* (lit)/Å
THF(II)	D_2O:THF:EO_d	17:1:0.5	6		17.2(4)	17.1(5)[a]
EO(II)	D_2O:TDF:EO	17:1:0.5	6			17.1(3)[b]
						17.2(7)[c]
						17.31[d]
						17.18[e]
DX(II)	D_2O:DX	17:1	0	−3[f]	17.1(9)	17.0(9)[a]
						17.1(0)[b]
CP(II)	D_2O:CP	17:1	11	7.2[g]	17.1(5)	
CB(II)	D_2O:CB	17:1	4	0[h]	17.2(2)	17.1(4)[a]
						17.0(9)[b]
PO(II)	D_2O:PO	17:1	0	−4.4[i]	17.2(3)	17.1(0)[b]
TMO(II)	D_2O:TMO	17:1	−9 to −5	−13.1[i]	17.1(2)	17.(1)[b]
					12.0(4)	
TMO(I)	D_2O:TMO	$7^{2/}{}_3$:1	−21 to −11	−20.8[i]	11.9(8)	12.0(2)[j]
						12.1(5)[j]
EO(I)	D_2O:EO	$7^{2/}{}_3$:1	14	12.3[k]	11.9(1)	11.89(1)[l]

[a] Bertie, J. E.; Jacobs, S. M. *J. Chem Phys.* **1978**, *69* (9), 4105. [b] Sargent, D. F.; Clavert, L. D. *J. Phys. Chem.* **1966**, *70*, 2689. [c] Kessler, T. R. Dissertation, RWTH Aachen, 1993. [d] Mak, Th. C. W.; McMullan, R. K. *J. Chem. Phys.* **1965**, *42*, 2732. [e] v. Stackelberg, M.; Meuthen, B. *Z. Elektrochem.* **1958**, *62*,130. [f] Venkateswaran, A.; Easterfield, J. R.; Davidson, D. W. *Can. J. Chem.* **1967**, *45*, 8846. [g] Lippert, E. L., Jr.; Palmer, H. A.; Blankenship, F. F. *Proc. Okla. Acad. Sci.* **1950**, *31*,115. [h] Morris, B.; Davidson, D. W. *Can. J. Chem*. **1971**, *49*, 1243. [i] Hawkins, R. E.; Davidson D. W. *J. Phys*. C*hem.* **1966**, *70*, 284. [j] Gough, S. R.; Garg, S. K.; Davidson, D. W. *Chem. Phys.* **1974**, *3*, 239. [k] Mazzucchelli, A.; Armenante, R. *Gazz. Chim. Ital.* **1922**, *52*, 344. [l] Bertie, J. E.; Bartes, F. E.; Hendrieksen, D. K. *Can. J. Chem.* **1975**, *53*, 71.

TABLE 2: Fit Parameters of the Guest Molecules in the Clathrate Hydrates and Average Intramolecular Dipole−Dipole Distances $\langle r \rangle$

	$\langle r \rangle$/Å	s^2	$\tau_0^*/10^{-13}$ s $\tau_1^*/10^{-13}$ s	E_a/kJ mol^{-1} H_a/kJ mol^{-1}	β α	*A*	Δ[a]
THF(II)	1.71	0.6(1)	4.34(7)	4.0(8)	0.14(0)		0.10
DX(II)	1.74	0.3(3)	5.99(1)	2.7(9)	0.2(3)		0.10
CP(II)	1.69	0.8(1)	5.86(1)	2.6(5)	0.2(3)		0.093
TMO(II)	1.75	0.5(8)	9.04(6)	1.8(5)	0.2(4)		0.074
TMO(I)	1.75	0.1(9)	0.4(2)	11.(5)	0.3(6)	0.(3)	0.045
			31.(2)	4.5(6)	0.3(6)		
CB(II)	1.70	3.0(8)	8.7(3)	5.1(3)	0.1(1)	0.(1)	0.046
			81.2(0)	1.5(4)	0.0(1)		
PO(II)	1.79	0.6(7)	14.(5)	8.0(0)	0.(9)	0.(1)	0.057
			2.57(4)	3.4(7)	0.26(7)		
EO(I)	1.82	0.36(2)	8.54(6)	3.6(4)	0.17(3)		0.083
EO(II)	1.82	0.1(3)	30.(8)	2.9(3)	0.2(4)		0.12

[a] $\Delta = \{\{\sum_{i=1}^{n}[w_i(Y_{\mathrm{cal}_i} - Y_{\mathrm{obs}_i})]^2\}/\text{degrees of freedom}\}^{1/2}$: standard deviation of data.

protons of the guest molecule have to be included in the calculation of the average proton−proton distances. The calculated values are listed in Table 2.

The parameter s^2 is a measure of the deviation of the theoretically expected coupling constant from the experimentally observed coupling constant. This parameter corresponds to the generalized order parameter introduced by Lipari and Szabo[14] for fast internal motions. According to Henry and Szabo,[15] fast internal motions are stretching vibrations along the bonding vector and deformational vibrations that change the orientation of the bonding vector. In T_1 measurements deformational vibrations cause a reduction of the spectral density, which cannot be distinguished from a reduction of the coupling constant. For the short-time behavior of the time correlation function a very fast nonexponential decay is assumed, which results in a high-frequency contribution to the spectral density function. Since the area of this curve must be constant, the maximum of the relaxation rate versus inverse temperature curve is reduced. Doelle[16] attributes strong deviations from the coupling constants and consequently small s^2 data to ultrafast librational motions of the whole molecule in a liquid cavity. These motions adjoin the motions of rotational diffusion.

The asymmetric relaxation rate versus inverse temperature curves can be described in terms of a distribution of reorientational correlation times. Specifically, the distribution function of Davidson and Cole[17] is used:

$$g(\tau_c) = \frac{\sin(\beta\pi)}{\pi}\left(\frac{\tau_c}{\tau_0 - \tau_c}\right)^{\beta} \quad \text{for } 0 < \tau_c < \tau_0$$

$$g(\tau_c) = 0 \quad \text{for } \tau_c > \tau_0 \tag{4}$$

The time correlation function is then written as

$$y_2(\tau) = \frac{\langle Y_{2,m}(0)Y^*_{2,m}(\tau)\rangle}{\langle Y_{2,m}(0)Y^*_{2,m}(0)\rangle} = \int_0^\infty g(\tau_c)\, e^{-\tau/\tau_c}\, d\ln\tau_c \tag{5}$$

where $Y_{2,m}$ is the second-order spherical harmonic, a function of the angles θ and φ describing the position of the intramolecular proton−proton vector in the guest molecule with respect to the external magnetic field. The angles θ and φ are time-dependent because of the reorientational motion of the guest molecule in its cavity described by the correlation time τ_c. The Fourier transform of this time-correlation function is the spectral density j_{CD}:

$$j_{CD} = \mathrm{Re}\int_0^\infty y_2(\tau)\, e^{-i\omega\tau}\, d\tau$$

$$= \frac{\sin[\beta \arctan(\omega\tau_0)]}{\omega[1 + (\omega\tau_0)^2]^{\beta/2}} \tag{6}$$

The shape parameter β is a measure of the asymmetry of the

relaxation rate versus inverse temperature curve. For $\beta = 1$ the Davidson−Cole distribution function turns into the Poisson distribution specified by one correlation time. As a result, the Bloembergen−Purcell−Pound spectral density[18] and hence a symmetric curve are obtained. For the temperature dependence of the cutoff correlation time τ_0 we assume the activation law

$$\tau_0 = \tau_0^* \exp\left(\frac{E_a}{RT}\right) \tag{7}$$

The slope of the rising branch gives the activation energy E_a. The asymmetric relaxation rate versus inverse temperature curves are composed of the extreme-narrowing region ($\omega_0\tau_0 \ll 1$) and the frequency-dependent region ($\omega_0\tau_0 \gg 1$) with the limits

$$j_{CD} = \tau_0\beta \quad \text{for } \omega\tau_0 \ll 1$$

$$j_{CD}(\omega) = \frac{\sin\left(\beta\frac{\pi}{2}\right)}{\omega^{1+\beta}\tau_0^{\beta}} \quad \text{for } \omega\tau \gg 1 \tag{8}$$

The least-squares fits of these curves carried out by the Powell method[19] result in the adjustable parameters s^2, β, E_a, and τ_0^*.

If the relaxation rate versus inverse temperature curve consists of two local maxima, an additional fit parameter A is necessary, which weighs both maxima and may be interpreted as the mole fraction. On the assumption that both local maxima originate from distributions of correlation times, the spectral density is then given by

$$j_{CD} = A\frac{\sin[\beta \arctan(\omega\tau_0)]}{\omega[1 + (\omega\tau_0)^2]^{\beta/2}} + (1 - A)\frac{\sin[\alpha \arctan(\omega\tau_1)]}{\omega[1 + (\omega\tau_1)^2]^{\alpha/2}} \tag{9}$$

with

$$\tau_0 = \tau_0^* \exp\left(\frac{E_a}{RT}\right)$$

and

$$\tau_1 = \tau_1^* \exp\left(\frac{H_a}{RT}\right)$$

α, H_a, and τ_1^* are additional fit parameters and equivalent to the parameters β, E_a, and τ_0^*. The fit parameters of the guest species in the different clathrate hydrates are summarized in Table 2.

Results

In all relaxation rate versus inverse temperature curves shown in Figures 2−7, the 300 MHz relaxation rates measured between 125 and 263 K adjoin the low-temperature data at 60 MHz, as expected for the extreme-narrowing region.

The relaxation rates in the high-temperature region between about 200 and 263 K show a different Arrhenius behavior at lower temperatures. The lack of stability of the clathrates may be responsible for this because an insufficient crystallization gives rise to higher relaxation rates. A hint for a "premelting" region is also given by the temperature dependent X-ray diffraction patterns in which an increase of ice reflexes is observed with increasing temperature. On the other hand the motion of the lattice beginning at about 200 K may influence the rotational behavior of the guest molecules in their cavities and hence change the rotational barriers. The increase of the relaxation rates at high temperatures may also originate from spin−rotation interactions becoming effective especially for small molecules at high temperatures. Because of the uncertain origin and the complex interactions between guest and host, the relaxation rates at high temperatures were not taken into consideration for evaluation of the data.

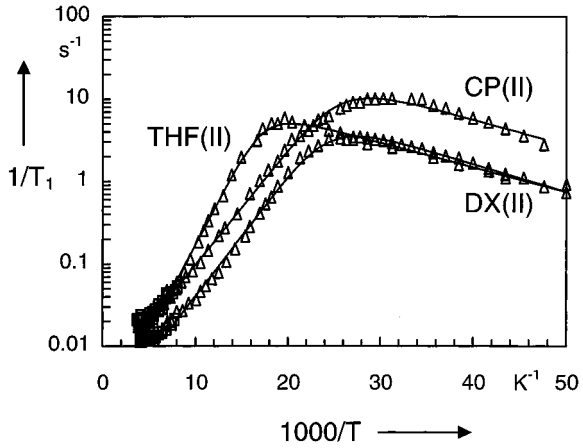

Figure 2. Proton relaxation rates $1/T_1$ of THF in the clathrate 1THF:$0.5EO_d$:$17D_2O$, of DX in the clathrate 1DX:$17D_2O$, and of CP in the clathrate 1CP:$17D_2O$ in the temperature range 20−260 K at frequencies of 300 MHz (□, 125−260 K) and 60 MHz (△, 20−154 K). The solid line is the theoretical curve based on a Davidson−Cole distribution.

The relaxation rate versus inverse temperature curve of THF in the clathrate 1THF:$0.5EO_d$:$17D_2O$ is shown in Figure 2. The relaxation behavior of THF at 60 MHz was already studied in the clathrates THF·D_2S·D_2O[20] and THF·D_2O.[7] The fit parameters ($E_a = 3.93$ kJ mol^{-1}, $\tau_0^* = 3.52 \times 10^{-13}$s, $\beta = 0.15$ for THF·D_2S·D_2O; $E_a = 4.14$ kJ mol^{-1}, $\tau_0^* = 3.75 \times 10^{-13}$ s, $\beta = 0.12$ for THF-D_2O) are in excellent agreement with the parameters calculated for the clathrate THF·EO_d·D_2O. Thus, we conclude that the EO_d molecules encaged in the pentagonal dodecahedra do not exert an influence on the rotational dynamics of the THF molecules.

The relatively large correlation time $\tau_0^* = 4.34 \times 10^{-13}$ s and the low activation energy of 4.08 kJ mol^{-1} found in the present work cause fast reorientation of the THF molecules in their cavities due to weak interactions between the guests and the D_2O molecules of the host lattice. In liquids the activation energies lie generally between 20 and 30 kJ mol^{-1} and the correlation times τ_0^* are about 10^{-16} s. Therefore, the fit parameters for the clathrate indicate that the rotational motion of the guests is hardly hindered energetically and the guest molecules collide about 1000 times less often with the cavity walls than the molecules do with each other in liquids. This high mobility of the guest molecules leads to the assumption that the motional process can no longer be described by the "small step" rotational diffusion. A hint in the same direction comes from dielectric relaxation studies.[9] The activation energy E_a(DR) = 3.80 kJ mol^{-1} agrees closely with the value E_a(NMR) = 4.08 kJ mol^{-1}. But the correlation time τ_0(DR) = 1.5×10^{-8} s at 43 K is about 2−3 times smaller than the value τ_0(NMR) = 3.9×10^{-8} s calculated for the same temperature. This discrepancy also shows that the guest molecules do not obey the diffusion process because in that case the following relation should hold: τ_0(DR) = $3\tau_0$(NMR). To point out the reorientational mobility for THF in different media, it is interesting to compare the correlation times of THF in pure liquid ($\tau = 1.61 \times 10^{-12}$ s) in a mixture with water ($\tau = 9.24 \times 10^{-12}$ s; mole fraction of 1:17), in the clathrate hydrate ($\bar{\tau} = \beta\tau_0 = 4.58 \times 10^{-13}$ s; extrapolated to 243 K by means of the Arrhenius relation), and in the gaseous state ($\tau_{free} = 3.93 \times 10^{-13}$s) at 243 K, a temperature point in the extreme-narrowing region. The THF molecules rotate much faster (factor of 20)

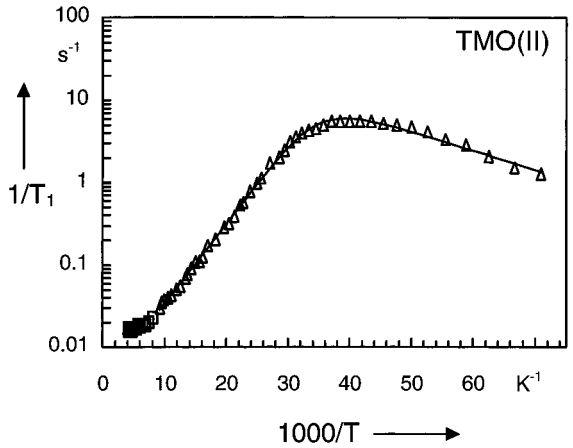

Figure 3. Proton relaxation rates $1/T_1$ of TMO in the clathrate 1TMO:$17D_2O$ in the temperature range 14−249 K at frequencies of 300 MHz (□, 125−249 K) and 60 MHz (△, 14−153 K). The solid line is the theoretical curve based on a Davidson−Cole distribution.

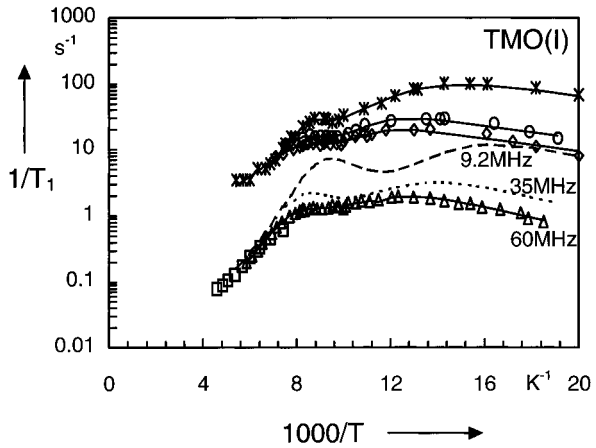

Figure 4. Proton relaxation rates $1/T_1$ of TMO in the clathrate 1TMO:$7^2/_3D_2O$ in the temperature range 54−218 K at frequencies of 300 MHz (□, own data at 135−218 K), 60 MHz (△, own data at 54−171 K; ◇, ref 10), 35 MHz[10] (○), and 9.2 MHz (*, ref 10). The solid line is the theoretical curve based on a Davidson−Cole distribution. The dotted line (35 MHz) and dashed line (9.2 MHz) are theoretical curves simulated with the parameters obtained from the fit at 60 MHz.

in the clathrate than in the liquid mixture because of a hydrogen-bonded network between water and THF in the liquid. The lack of hydrogen bonds also ensures the THF molecules being faster in the pure liquid than in the mixture with water. By comparison of the correlation times for the clathrate and for free rotation, it can be stated that the reorientation of THF in the clathrate approaches the value for free rotation at high temperatures. For THF in the gaseous state the function of τ_{free} is proportional to $(1/T)^{1/2}$, while the correlation times for the clathrate increase exponentially with decreasing temperatures.

The relaxation rate versus inverse temperature curve of DX in the clathrate 1DX:$17D_2O$ (see Figure 2) is similar to that for the clathrate THF(II). The maximum is shifted by about 10 K to lower temperatures. The exchange of a CH_2 group by oxygen in DX leads to an activation energy one-third smaller than the value for THF and a correlation time τ_0^* about one-third higher. As a consequence, the reorientation of DX is energetically less restricted in the temperature region between 40 and 200 K and the DX molecules collide less often with the lattice walls.

In Figure 2 also the relaxation rate versus inverse temperature curve of CP in the clathrate 1CP:$17D_2O$ is shown. For CP, the only nonpolar molecule of all studied guest compounds, the maximum is about 10 K lower than that for DX. The fit parameters E_a, τ_0^*, and β agree with those for DX. Consequently, CP reorientates as fast as DX does. From NMR relaxation studies at 9.2 MHz Davidson and Ripmeester[10] calculated an activation energy of 2.67 kJ mol^{-1} corresponding to the value for 60 MHz. The maximum of this curve lies at 29 K as expected for measurements at a lower frequency.

In comparison with the five-membered rings THF, DX, and CP the reorientational motion of the four-membered ring TMO in the clathrate 1TMO:$17D_2O$ (see Figure 3) is hindered much less and the lower activation energy is also connected with a higher correlation time τ_0^*. The activation energy agrees with the value of 1.92 kJ mol^{-1} from dielectric relaxation studies[21] and NMR measurements at 9.2 MHz.[10] The maximum of the curve occurs at 25 K. The high mobility of this guest molecule is possibly attributed to the small size of TMO. By reference to the X-ray diffraction experiment, the pattern of the clathrate TMO(II) is composed of structure II as well as of structure I reflexes. Therefore, the relaxation rates reflect the reorientation of the guest molecules in both the hexakaidecahedra and the tetrakaidecahedra. Since the motions of the TMO molecules in structure I are nearly frozen at 50 K, the relaxation rates for the mixed clathrate should deviate from the fitted curve in the temperature range between 50 and 230 K. However, the data points between 33 and 230 K yield a straight line. Therefore, we conclude that TMO is mostly encaged in the hexakaidecahedra of structure II and that the relaxation due to the reorientation in the tetrakaidecahedra of structure I can be neglected.

In contrast to the clathrate TMO(II), the relaxation rate versus inverse temperature curve of TMO in the clathrate 1TMO:$7^2/_3D_2O$ (see Figure 4) shows two maxima, each of which are fitted with the spectral density by Davidson−Cole. The fit parameter A weighing the two maxima has a large error of ±0.3. The left maximum is associated with a higher activation energy and a lower correlation time τ_0^* compared to the right one. The shape parameter β is the same for both partial fits. But its value for the high-temperature maximum is not as well-defined because of the superimposed curves. By comparison of the reorientation of the clathrates TMO(I) and TMO(II), the mobility of the guest molecule is less in the tetrakaidecahedra than in the hexakaidecahedra. In addition, a flattening of the relaxation rate versus inverse temperature curve is observed below 50 K. As Albayrak et al.[7] showed for the clathrate 1THF:$17D_2O$, the flattening of the curve below about 20 K is described by a coupled ensemble of quantum mechanical hindered rotators where the reorientation rate shows a distribution that can be represented by a Davidson−Cole function. These low-frequency librations in the region where the temperature dependence of the nuclear spin relaxation rate deviates from the Arrhenius law $1/T_1 \propto \tau_0^{-\beta} = (\tau_0^*)^{-\beta} \exp(-\beta E_a/(kT))$ are not examined further in this paper. To test the quality of the fitting procedure, we tried to fit also the temperature-dependent data at 60, 35, and 9.2 MHz published by Davidson and Ripmeester.[10] Unfortunately, we could not read the data points with the necessary accuracy from the corresponding diagram of the original publication. Furthermore, we do not know the error bars of these data and of the fit parameters. Therefore, we compare these data only qualitatively. In Figure 4 the results of the simulated curves at 35 and 9.2 MHz (dashed and punctured lines) are also shown. They were calculated using the fit parameters of the 60 MHz data. The literature data show a similar tendency for the experimental and simulated curves. But the relaxation rates are shifted to higher values presumably because of uncompleted crystallization or the presence of paramagnetic oxygen in the sample. Two absorption maxima are also confirmed by dielectric studies,[10,22] where the first peak is connected with an activation energy of 8.8 kJ mol^{-1} and the

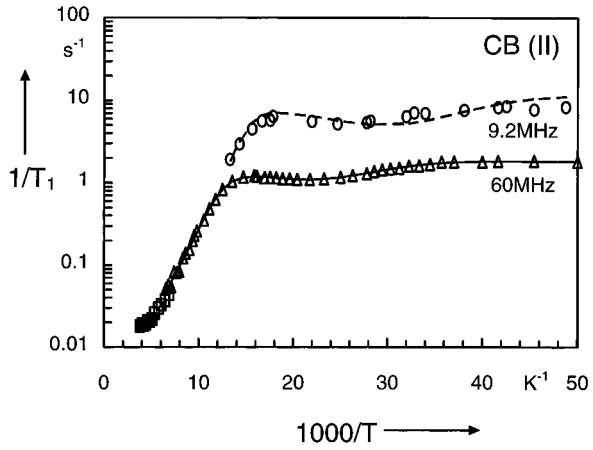

Figure 5. Proton relaxation rates $1/T_1$ of CB in the clathrate 1CB:$17D_2O$ in the temperature range 20−263 K at frequencies of 300 MHz (□, own data at 146−263 K), 60 MHz (△, own data at 20−153 K), and 9.2 MHz (○, ref 10). The solid line is the theoretical curve based on a Davidson−Cole distribution. The dashed line is the theoretical curve simulated with the parameters obtained from the fit at 60 MHz.

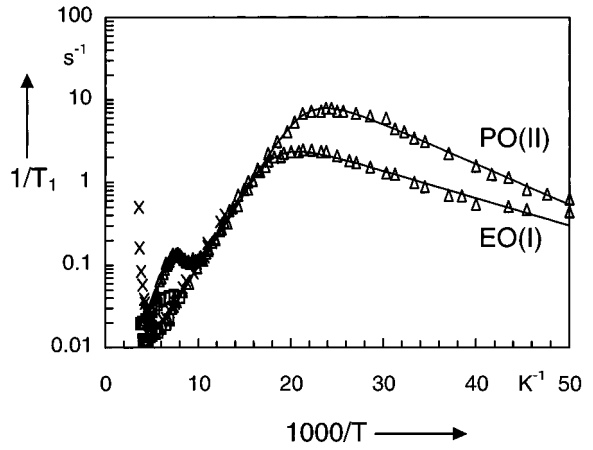

Figure 6. Proton relaxation rates $1/T_1$ of EO in the clathrate 1EO:$7^2/_3D_2O$ and of PO in the clathrate 1PO:$17D_2O$ in the temperature range 20−263 K at frequencies of 300 MHz (□, 133−263 K), 60 MHz (△, 20−203 K), and 30 MHz (×, ref 8). The solid line is the theoretical curve based on a Davidson−Cole distribution.

second peak with 0.58 kJ mol^{-1}. The existence of an ordering transition is also shown by measurements of the second moments. With regard to NMR studies Davidson and Ripmeester[10] assign the major peak to reorientation of TMO about its polar axis aligned along the $\bar{4}$ axis of the cage. The peak at lower temperatures is of less certain origin. It may arise from the relatively rapid reorientation or partial reorientation of a fraction of the TMO molecules that are not aligned along the $\bar{4}$ axis. Although evidence or the existence for a "partial" ordering transition in structure I is thus provided by three kinds of different experiments, the infrared spectrum[23] shows no such indication.[10]

The relaxation rate versus inverse temperature curve of CB in the clathrate 1CB:$17D_2O$ (see Figure 5) is also composed of two superimposed asymmetric curves. Both maxima at 66 and 23 K are fitted by using eq 9. By comparison of the activation energies and the correlation times τ_0^* and τ_1^* with each other, the reorientation of the dipoles is considerably slower in the high-temperature region than in the low-temperature region. The extremely small distribution parameters signify an unusual broad distribution of correlation times, where the faster motion is connected with the lower β-value. The presence of two broad distributions of correlation times for CB was also found by Davidson and Ripmeester,[10] who studied the relaxation behavior of CB at 9.2 MHz. Their data points fall on the simulated curve (dashed line), which was calculated from the fit parameters obtained from the 60 MHz data points. In earlier ϵ'' dielectric measurements[24] only one reorientational process with an activation energy of 6.02 kJ mol^{-1} was observed. In comparison with the relaxation curves of THF(II), DX(II), CP(II), and TMO(II) the abnormal behavior of CB(II) is possibly attributed to the large ratio of cavity diameter to molecular diameter ($r = 1.01$), the large dipole moment ($\mu = 2.78$ D), and the aspherical geometry of CB. According to Davidson and Ripmeester,[10] rotation of the CB molecule about its long dipolar axis is responsible for the low-temperature peak, while much slower reorientation about the other axis gives rise to the high-temperature peak.

In the relaxation rate versus inverse temperature curve of PO in the clathrate 1PO:$17D_2O$ (see Figure 6) the two maxima indicate different motions. The peak in the high-temperature region at a maximum of 133 K is characterized by a relatively strong hindered motion with a low collision frequency of the guest molecule with the cage wall. In contrast to the other clathrates a high rotational barrier is connected with a high correlation time τ_0^*. At lower temperatures faster motions are still present. They are described by fit parameters that are typical for the cyclic guest compounds presented in this paper. The maximum of the second peak lies at 42 K. Since PO is the only guest molecule with a methyl group perpendicular to the epoxy ring, it is quite intriguing to assign the maxima to the motion of the molecule with internal rotation of the methyl group. In this special case the fit parameter A corresponds to the generalized order parameter S^2 introduced by Lipari and Szabo[14] for overall motion with internal rotation. On the assumption that the methyl group rotates faster than the molecule, the maximum in the high-temperature region is responsible for the overall motion, while the fast internal rotation gives rise to the maximum in the low-temperature region. This assignment is not compelling, since studies of the methyl group rotation have proven that the rotational barriers of methyl groups in clathrate hydrates may be different from those in gaseous or solid states.[25,26] As a result, it turned out that the geometry of the guest molecule as well as of the cavity plays a key role for the magnitude of activation energies. From the present experiment it is not possible to assign the peaks, since the measured NMR signal is an average of all relaxing protons in the molecule.

The guest molecule EO in the clathrate 1EO:$7^2/_3D_2O$ is encaged to 90% in the tetrakaidecahedra. It is expected that a small fraction, approximately 10%, is also enclathrated in the pentagonal dodecahedra.[27,28] The fit parameters of the fitted relaxation rate versus inverse temperature curve (see Figure 6) are of the same order of magnitude as those for the clathrates THF(II), DX(II), CP(II), and TMO(II). In contrast to the clathrate TMO(I) in which the TMO molecules are encaged in the tetrakaidecahedra as well, the curve of the clathrate EO(I) shows only one maximum at 48 K. In addition the motions of TMO in the tetrakaidecahedra are restricted to librational oscillations at 50 K, while at the same temperature the curve of the clathrate EO(I) has just reached the maximum. The different reorientational behavior of EO and TMO encaged in the same cavity is attributed to the different molecular sizes (EO(I), $d_{guest}/d_{cage} = 0.90$; TMO(I), $d_{guest}/d_{cage} = 0.96$). Hayward and Packer[8] carried out T_1 measurements on the same EO clathrate at 30 MHz in the temperature range between 77 and 279 K. In the temperature region between 77 and 193 K the data points are in excellent agreement with the relaxation rates at 60 MHz, as expected. The authors calculate an activation energy of 3.74

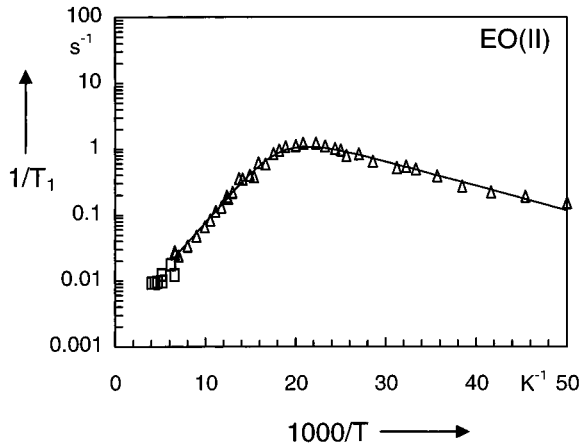

Figure 7. Proton relaxation rates $1/T_1$ of EO in the clathrate 1TDF:0.5EO:17D_2O in the temperature range 20−253 K at frequencies of 300 MHz (□, 163−253 K) and 60 MHz (△, 20−152 K). The solid line is the theoretical curve based on a Davidson−Cole distribution.

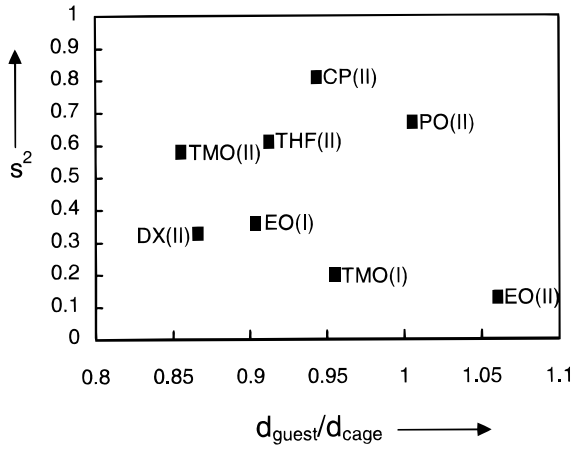

Figure 8. Dependence of the fit parameter s^2 on the ratios of guest molecule diameter to cage diameter.

kJ mol^{-1} but a markedly lower correlation time of $\tau_0^* = 6.76 \times 10^{-14}$ s. The steep increase of the rates between 193 and 279 K presumably originates from incomplete crystallization and hence from instability of the clathrate as discussed earlier for 1THF:17D_2O.[7] Whereas dielectric studies[28] on the clathrate EO(I) give rise to an activation energy of 5.86 kJ mol^{-1}, Ripmeester[27] calculated an activation energy of 3.73 kJ mol^{-1} obtained from NMR deuterium measurements of EO_d. As a possible explanation for this discrepancy, the author suggests that the lower value reflects reorientations about the polar EO axis that the dielectric method does not detect. Davidson and Ripmeester[10] state that ordering of the guest's dipole direction in structure I along the $\bar{4}$ axis of the tetrakaidecahedra is possible. But the dielectric and nuclear magnetic data of the encaged ethylene oxide show no sign of an ordering transition.

According to Fleyfel and Delvin,[12] the guest molecule EO in the clathrate 1TDF:0.5EO:17D_2O (see Figure 7) is encaged in the pentagonal dodecahedra of structure II. Since the stoichiometry provides complete occupation of all hexakaidecahedra with TDF molecules, EO is not enclathrated in the large cavities. In comparison with EO encaged in the tetrakaidecahedra of structure I the activation energy is lower and the correlation time τ_0^* is larger. This results in a slower reorientation of the guest molecules in the pentagonal dodecahedra. The maximum of the relaxation rate versus inverse temperature curve occurs at 48 K as well. Although EO fits tightly in the small cavity ($d_{guest}/d_{cage} = 1.06$), the curve does not consist of two local maxima, since it is observed for guest molecules with similar diameter ratios. We assume that both the shape of the guest molecule and the geometry of the cavity are responsible for the existence of only one maximum in the curve. Since EO is more spherical as CB and PO, these molecules carry out a more anisotropic reorientation whose faster motion is still visible at low temperatures. The influence of the cage geometry on the reorientational motion becomes clear by regarding the free space of the guest molecules, which is restricted within the cages. Whereas the tetrakaidecahedra force TMO molecules in preferred orientations because of the aspherical form of this cage, the pentagonal dodecahedra with a nearly spherical geometry do not give rise to an ordering of the EO molecules.

Discussion

The fits of the relaxation rates to equations for intramolecular dipole−dipole interactions result in s^2 values being less than 1 except for the clathrate CB(II). The value of $s^2 = 3.08$ for CB encaged in the hexakaidecahedra indicates that interactions other than the intramolecular dipole−dipole interactions contribute to the relaxation process. Intermolecular interactions between the guest molecule and the deuterons of the lattice molecules would shift the maximum of the relaxation rate versus inverse temperature curve to higher rates and hence to a smaller s^2 value. With a minimal distance of 2.30 Å between the protons of CB and the deuterons of the lattice we obtain a s^2 value of 1.23, which is much closer to 1.

For the remaining clathrates the different s^2 values are discussed in view of the ratios of guest diameter to cage diameter because librational motions of the guest molecules that give rise to varying s^2 values are influenced by the space available for rotating molecules (see Figure 8). By comparison of EO enclathrated on one hand in the tetrakaidecahedra of structure I and on the other hand in the pentagonal dodecahedra of structure II, it can be stated that a smaller cavity gives rise to a smaller s^2 value. The same effect is observed regarding the clathrates TMO(I) and TMO(II). Therefore, we conclude that fast librational motions show up if the mobility of the guest molecule is restricted by the cavity.

The parameters s^2 of the clathrates DX(II), THF(II), and CP(II) show the opposite trend. Despite less space for the guest molecules, the s^2 values increase. For these guest molecules oxygen atoms present in the molecule play the decisive role, yielding increasing s^2 values with decreasing numbers of oxygen atoms.

The shape parameter β represents a fit parameter resulting from the analytical spectral density by Davidson−Cole. Broad distributions of correlation times are typical for the reorientations of the guest molecules in clathrate hydrates. There is no straightforward correlation among the different β-values and molecule-dependent properties such as dipole moment, moment of inertia, and diameter ratio. The nature of the cavity also has no apparent influence on the size of β because the shape parameter changes by varying the guest molecules encaged in the same cavity as well as the cavities containing the same guest molecule. However, the presence of a shape parameter can be explained in the following way. If the rotational motions of the guest molecules cannot be described by "small-step"-rotational diffusion, the necessary condition of a Markov process is no longer met. Stochastic processes with a "memory" result in a nonexponential correlation function and hence in an asymmetric relaxation rate versus inverse temperature curve. For free rotation a nonexponential time-correlation function is obtained.[29] Thus, it is possible to explain a shape parameter

smaller than 1 as a result of rotational dynamics determined by inertial motion. Another possibility for explaining the small shape parameters is given by Garg et al.,[9] who assume a heterogeneous distribution of correlation times. The origin of this distribution is thought to lie in the disorder of the reorientations of the water molecules. As a result of the 6 possible orientations of each of the 28 water molecules that make up the hexakaidecahedron, there is a wide variation in direction and magnitude of the resultant electrostatic fields within the cage.[11] The authors state that in the case of polar guest molecules, this leads to considerable variability among the energies of preferred orientations and in turn to a wide distribution of modes and rates of reorientation. We do not agree with this statement because the X-ray diffraction patterns show sharp reflexes, proving that clathrate hydrates are crystalline and not amorphous solids. Therefore, different orientations of the guest molecules should not cause such a strong deviation of the distribution parameter β from 1. Considering further that the Davidson−Cole distribution is a logarithmic function of the correlation time, the correlation times of the guest molecules in different surroundings should differ very strongly in order to explain the small β values found in the clathrate hydrates.

To compare the different mobilities for the guest molecules in their cages, we calculated the average correlation times $\bar{\tau} = \tau_0\beta$ from the fit parameters E_a, τ_0^*, and β at 90 K. At this temperature the correlation times of the guest molecules are in the "extreme-narrowing" region except for TMO(I). At 90 K the slower motions are nearly frozen in the clathrates PO(II) and TMO(I), while the fast motion in the clathrate CB(II) is not yet apparent in the relaxation rates. Therefore, these motions cannot be included in the following discussion. The correlation times $\bar{\tau}$ lying between 2.57×10^{-12} s for the clathrate TMO(II) and 4.97×10^{-10} s for the clathrate TMO(I) reflect the different strengths of the interactions between the guest molecules and the host lattice. Apart from van der Waals interactions, electrostatic interactions play an additional role for polar guest molecules. Therefore, we found it worthwhile to connect the average correlation times $\bar{\tau}$ with molecule-dependent properties such as dipole moment, moment of inertia, and diameter ratio.

These studies include literature data of 1,4-dioxane clathrates, which were obtained from proton relaxation measurements at 9.2 MHz.[30] We calculated an average correlation time $\bar{\tau}$ of 2.38×10^{-10} s from the parameters given by the authors.

Davidson and Ripmeester[10] have found from dielectric measurements that the reorientation times of the cage water molecules decrease with increasing dipole moments of the guest molecules. Because of electrostatic interactions between host and guest, the reorientational motions of the guest molecules should also depend on their dipole moments. Although the dielectric relaxation times are related to the decay of the autocorrelation function of the dipole moments, while the nuclear magnetic correlation times reflect the reorientational motions of the proton−proton vector, both times should be comparable if both vectors reorient similarly. Therefore, a comparison of the nuclear magnetic correlation times $\bar{\tau}$ with the dipole moments of the guest molecules is meaningful. However, a correlation between both quantities is not found.

Figure 9 shows how a change of the ratios of guest diameter to cage diameter affects the correlation times $\bar{\tau}$. With increasing restriction of space, the reorientations of the guest molecules TMO, DX, THF, CB, and 1,4-dioxane enclathrated in the hexakaidecahedra of structure II become slower. The clathrate PO(II) does not join this trend because the reorientational motion of PO is split into two components, in contrast to the guest molecules mentioned above. The fast motion of PO is visible

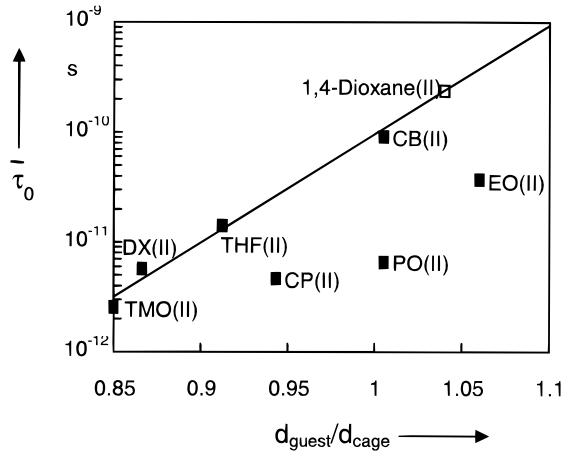

Figure 9. Dependence of the average correlation times $\bar{\tau}_0 = \beta\tau_0$ calculated at 90 K on the ratios of guest molecule diameter to cage diameter (semilogarhithmic plot). The solid line indicates the trend.

only at 90 K, while the slower motion is nearly frozen at this temperature. The clathrate CP(II) is also exceptional if compared to the correlation times $\bar{\tau}$ of the clathrates THF(II) and CB(II). Despite the small free space within the cavities available for this guest, the relatively high mobility of CP may be attributed to the fact that for nonpolar guest molecules only van der Waals interactions play a role and that no oxygen atoms are present in the molecule. The correlation times $\bar{\tau}$ of the clathrates EO(I), TMO(I), and EO(II) deviate from the trend found for the clathrates TMO(II), DX(II), THF(II), CB(II), and 1,4-dioxane(II) because the guest molecules are encaged in different cavities. For nearly the same diameter ratios EO rotates somewhat more slowly in the tetrakaidecahedra as THF does in the hexakaidecahedra. A comparison of the clathrates EO(I) and TMO(I) confirms that the correlation times $\bar{\tau}$ increase as soon as the space available for reorientation is restricted. But the motions of the guest molecules encaged in the holes of structure I are generally slower than those encaged in the large cavities of structure II. For EO enclathrated in the pentagonal dodecahedra of structure II a correlation time is calculated that is specific for this cavity type. It is true that the correlation time of EO is twice as large in the smaller cavity of structure II as it is in the larger tetrakaidecahedra of structure I, but it is much too small with regard to the fact that EO fits in the small cavities only with distortion of the pentagonal dodecahedra.

For reorientational motions in the liquid the geometry of the molecule is decisive in describing diffusional processes. By comparison, the dynamics in the gaseous state is determined by the moments of inertia. For the reorientations of the guest molecules in clathrate hydrates the moment of inertia may gain increasingly in importance. The plot of the correlation times $\bar{\tau}$ versus the square of the average moments of inertia (see Figure 10) shows for the clathrates TMO(II), PO(II), THF(II), CB(II), and 1,4-dioxane(II) a good correlation. CP is an exception presumably because of its nonpolarity. Despite the larger moment of inertia, it rotates markedly faster than THF. But the absence of polarity does not appear to be the only reason for the fast reorientation of CP because the rotation of 1,4-dioxane, the dipole moment of which is nearly zero because of the special conformation in the hydrate,[30] is more hindered than it is for CP. The presence of oxygen atoms in the molecule appears to affect the reorientational behavior of the guest molecule decisively. The correlation between moments of inertia of the guests and their correlation times $\bar{\tau}$ is a further hint of nondiffusive reorientational processes of the guest compounds in clathrate hydrates.

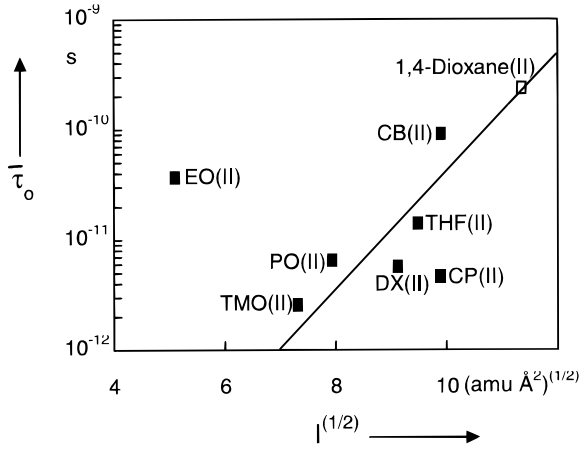

Figure 10. Dependence of the average correlation times $\bar{\tau}_0 = \beta\tau_0$ calculated at 90 K on the moments of inertia of the guest molecules (semilogarithmic plot). The solid line indicates the trend.

Conclusions

Summing up, we have shown that for nine different clathrate hydrates the Davidson−Cole spectral density is a suitable function for fitting the NMR proton relaxation rates of the guest molecules in the temperature region between 20 and 200 K. With the exception of the clathrate CB(II) the maxima of the asymmetric relaxation rate versus inverse temperature curves are smaller than expected from the structural data of the guest molecules. This discrepancy is expressed as a parameter s^2, which is smaller than 1. Small s^2 values are attributed to fast librational motions, which are expected if the motion of the guest molecule is restricted by the cavity. The shape parameter β in the Davidson−Cole spectral density with an average value of 0.22 indicates a broad distribution of correlation times. In comparison to liquids the reorientations of the guest molecules are generally connected with small activation energies. The large correlation times τ_0^* representing the prefactors of the Arrhenius equation show that the molecules collide less often with the cavity walls than the molecules do with each other in liquids. Therefore, the rotational dynamics of the guest compounds cannot be described by the "small-step"-rotational diffusion.

We also conclude that a simple correlation between the average correlation times $\bar{\tau}$ and molecule-dependent properties such as dipole moment, moment of inertia, and diameter ratio does not exist. The different cage geometries of the hexakaidecahedra, tetrakaidecahedra, and pentagonal dodecahedra give rise to a characteristic reorientational behavior of the guest molecule. However, a trend is observed for different guest molecules encaged in the hexakaidecahedra of structure II. The correlation times $\bar{\tau}$ show a tendency to increase with increasing molecular sizes and moments of inertia. The dipole moment only plays a secondary role. The guest molecule CP is exceptional; the low correlation time $\bar{\tau}$ of the relatively large CP molecule is possibly attributed to the nonpolarity of the guest and to the lack of oxygen atoms.

It is known that conformational motions of the cyclic molecules also lead to changes of correlation times. The contribution of conformational changes to the rotational motions cannot be appreciated by the experiments performed in this paper. However, conformational motions may be responsible for the scattering of the data.

Acknowledgment. We thank Professor W. Bronger and Dr. P. Müller, Institut für Anorganische Chemie der RWTH Aachen, for carrying out the X-ray diffraction experiments, as well as Dr. R. Küchler, Institut für Physik der Universität Dortmund, for making available the 60 MHz spectrometer.

References and Notes

(1) Franks, F. *Water - A comprehensive treatise;* Plenum Press: New York, 1973; Vol. 2.
(2) Sloan, E. D., Jr. *Clathrate Hydrates of Natural Gases;* Marcel Dekker: Inc.: New York, 1990.
(3) Tanaka, H.; Kiyohara, K. *J. Chem. Phys.* **1993**, *98*, 8110.
(4) v. Stackelberg, M.; Müller, H. R. *Z. Elekrochem.* **1954**, *58*, 25.
(5) v. Stackelberg, M.; Jahns, W. *Z. Elektrochem.* **1954**, *58*, 162.
(6) Ripmeester, J. A.; Ratcliffe, C. I. In *Inclusion Compounds*; Atwood, J. L., Davies, J. E. D., MacNicol, D. D., Eds.; Oxford University Press: Oxford, 1991; Vol. 5, Chapter 2.
(7) Albayrak, C.; Zeidler, M. D.; Küchler, R.; Kanert, O. *Ber. Bunsen-Ges. Phys. Chem.* **1989,** *93*, 1119.
(8) Hayward, R. J.; Packer, V. J. *Mol. Phys.* **1973**, *25*, 1443.
(9) Garg, S. K.; Davidson, D. W.; Ripmeester, J. A. *J. Magn. Reson.* **1974**, *15*, 295.
(10) Davidson, D. W.; Ripmeester, J. A. In *Inclusion Compounds*; Atwood, J. L., Davies, J. E. D., MacNicol, D. D., Eds.; Academic Press: New York, 1984; Vol. 3, Chapter 3.
(11) Davidson, D. W. *Can J. Chem.* **1971**, *49*, 1224.
(12) Fleyfel, F.; Delvin, J. P. *J. Phys. Chem.* **1988**, *92*, 631.
(13) Sargent, D. F.; Calvert, L. D. *J. Phys. Chem.* **1966**, *70*, 2689.
(14) Lipari, G.; Szabo, A. *J. Am. Chem. Soc.* **1982**, *104*, 4559.
(15) Henry, E. R.; Szabo, A. *J. Chem. Phys.* **1985**, *82*, 4753.
(16) Dölle, A. Unpublished results.
(17) Davidson, D. W.; Cole, R. H. *J. Chem. Phys.* **1951**, *19*, 1484.
(18) Bloembergen, N.; Purcell, E. M.; Pound, R. V. *Phys. Rev.* **1948**, *73*, 679.
(19) Powell, M. J. D. *A FORTRAN Subroutine for Solving System of Nonlinear Algebraic Equations*; Gordon & Breach Science Publishers: New York, 1970.
(20) Kessler, T. R. Ph.D. Dissertation, Rheinisch-Westfälische Technische Hochschule Aachen, Aachen, Germany, 1993.
(21) Gough, S. R.; Hawkins, R. E.; Morris, B.; Davidson, D. W. *J. Phys. Chem.* **1973**, *77*, 2969.
(22) Gough, S. R.; Garg, S. K.; Davidson, D. W. *Chem. Phys.* **1974**, *3*, 239.
(23) Bertie, J. E.; Jacobs, S. M. *Can. J. Chem.* **1977**, *55*, 1777.
(24) Morris, B.; Davidson, D. W. *Can. J. Chem.* **1971**, *49*, 1243.
(25) Ripmeester, J. A. *J. Chem. Phys.* **1978**, *68*, 1835.
(26) Ripmeester, J. A. *Can. J. Chem.* **1982**, *60*, 1702.
(27) Ripmeester, J. A. *Can. J. Chem.* **1976**, *54*, 3677.
(28) Garg, S. K.; Morris, B.; Davidson, D. W. *J. Chem. Soc., Faraday Trans. 2* **1972**, *68*, 481.
(29) Steele, W. A. *J. Chem. Phys.* **1963**, *38*, 2411.
(30) Gough, S. R.; Ripmeester, J. A.; Davidson, D. W. *Can. J. Chem.* **1975**, *53*, 2215.